First-principles simulations of the stretching and final breaking of Al nanowires: Mechanical properties and electrical conductance

Pavel Jelínek,[1,2] Rubén Pérez,[1] José Ortega,[1] and Fernando Flores[1]
[1]*Departamento de Física Teórica de la Materia Condensada, Universidad Autónoma de Madrid, E-28049 Spain*
[2]*Institute of Physics, Academy of Sciences of the Czech Republic, Cukrovarnická 10, 1862 53,Prague, Czech Republic*
(Received 21 November 2002; revised manuscript received 23 January 2003; published 13 August 2003)

The evolution of the structure and conductance of an Al nanowire subject to a tensile stress has been studied by first-principles total-energy simulations. Our calculations show the correlation between discontinuous changes in the force (associated with changes in the bonding structure of the nanowire) and abrupt modifications of the conductance as the nanowire develops a thinner neck, in agreement with the experiments. We reproduce the characteristic increase of the conductance in the last plateau, reaching a value close to the conductance quantum $G_0=2e^2/h$ before the breaking of the nanowire. A dimer defines the contact geometry at these last stages, with three channels (one dominant) contributing to the conductance.

DOI: 10.1103/PhysRevB.68.085403 PACS number(s): 73.63.−b, 62.25.+g, 73.63.Rt, 68.65.−k

I. INTRODUCTION

The electrical and mechanical properties of metallic nanowires have received a lot of attention.[1] Although point contacts have been studied for many years, it is only recently that the gentle control of the distance between two metals using a scanning tunneling microscope (STM)[2,3] or a mechanically controlled breaking junction (MCBJ)[4] has allowed the experimental characterization of atomic contacts and the observation of quantum effects in both the conductance and the forces.[2] In a pioneering work, Scheer *et al.*[5] have shown, analyzing the superconducting properties of an atomic contact, how the transport properties of the system just before the breaking point depend on a few channels that they related to the atomic orbitals of the contact.

The formation of necks and atomic contacts in stretched metallic nanowires has been analyzed theoretically using different approaches. Nanowire deformation can be studied by molecular dynamics simulations using either classical[6,7] or effective-medium theory potentials.[8,9] First-principles calculations based on density functional theory[10–13] (DFT) provide a more accurate description of the mechanical properties and the electronic structure needed for the calculation of the conductance, but the large computational demand restricts most of the applications to an analysis of the model geometries for the contact (e.g., monoatomic chains). To our knowledge, the most complete calculation of the deformation of a metallic nanowire has been presented by Nakamura *et al.*,[14] who analyzed, using DFT calculations, a Na nanowire with 39 atoms. In this simulation, the wire is elongated in steps of 0.2 or 0.4 Å until it reaches the breaking point. The conductance is determined using the Landauer-Buttiker formula, where the transmission matrix is calculated from the self-consistent electrostatic potential using scattering techniques.[15] This calculation showed how the nanowire deformation was accompanied by a rearrangement of the atomic configuration, which introduces also jumps in the forces and conductance of the system.

Addressing this complex problem with a fully converged first-principles description would be still too computationally demanding. One possibility is to stick to accurate plane-wave (PW) DFT methods, carefully relaxing the conditions for convergence[16] (basis set cutoff, *k*-point sampling, etc.). A second alternative is to resort to local orbital DFT methods, especially those devised with the aim of computational efficiency, which allow first-principles studies of much more complex systems. The formulation in terms of local orbitals has an added value, as the transport properties can be easily calculated from the resulting [tight-binding or linear combination of atomic orbitals (LCAO)] electronic Hamiltonian using nonequilibrium Green's function techniques.[17] Thus, efficient local-orbital DFT methods are probably the best available tools for a first-principles analysis of complex nanowires. In this work, we have studied the evolution of the structure and conductance of an Al nanowire as a function of the stretching by means of a fast local-orbital minimal basis DFT local density approximation (LDA) technique (FIREBALL96).[18,19] This technique offers a very favorable accuracy and efficiency balance if the atomiclike basis set is chosen carefully.[20] This approach is complemented with PW-DFT-LDA calculations [using CASTEP (Ref. 21)] performed at the critical points of the nanowire deformation, as discussed below. Closely related approaches,[22–26] based on the combination of *ab initio* calculations on local-orbital basis and Keldysh-Green function methods, have been recently applied to characterize some ideal geometries (mainly, atomic chains) for Al and Au nanowires.

II. MECHANICAL PROPERTIES: TOTAL ENERGY, FORCES, AND STRUCTURE

We have studied the system shown in Fig. 1(a), having 48 atoms—12 of them in the wire—embedded in an Al(111) surface having a (3×3) periodicity. We also impose periodic conditions in the direction perpendicular to the surface, joining artificially the last two layers of the system. The stretching of the system is simulated, increasing the distance between the two limiting layers by steps of 0.1 Å. After each step, the system is allowed to relax towards its configuration

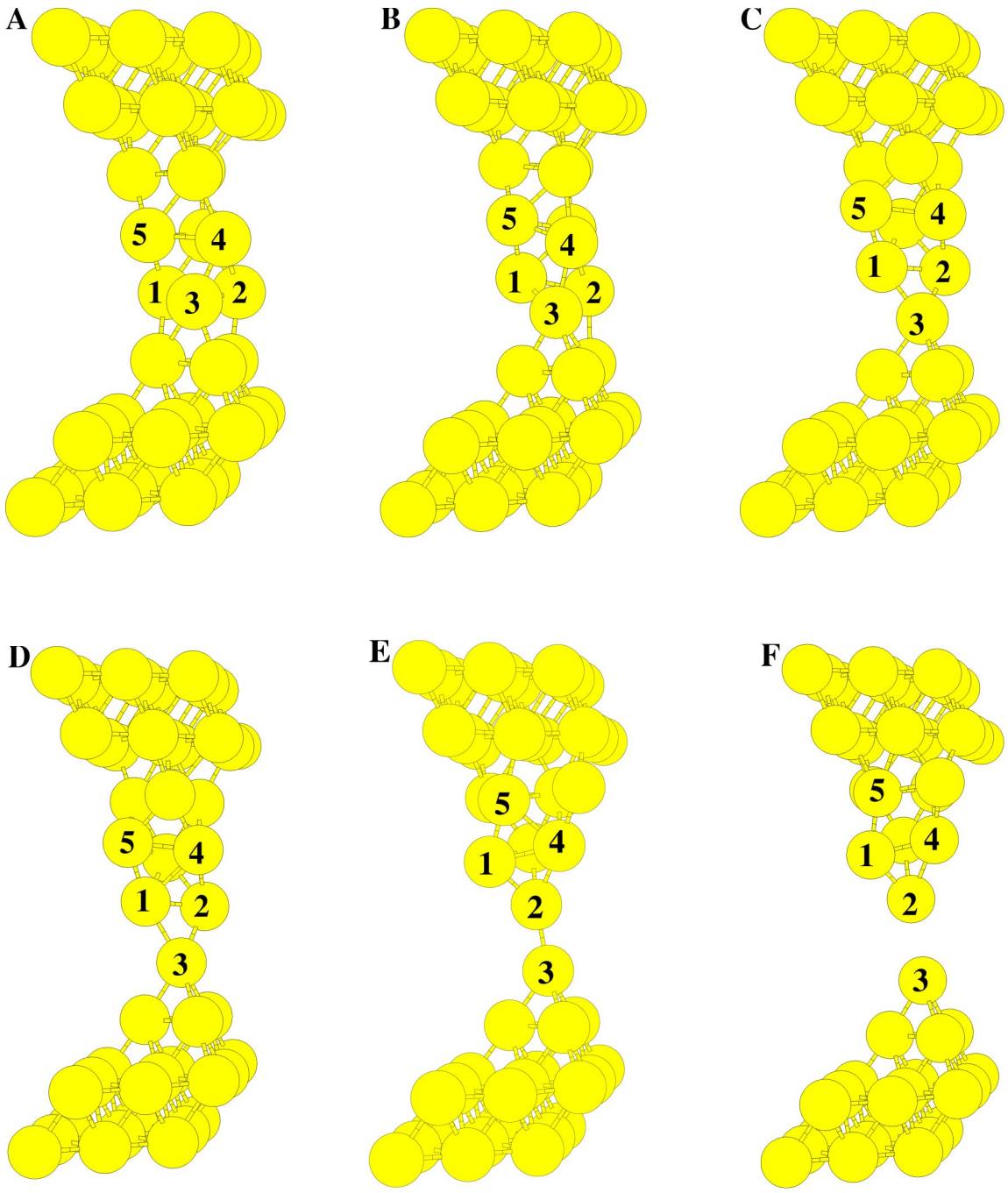

FIG. 1. (Color online) Ball-and-stick model of the structure of the Al nanowire for different steps of the stretching process (see Fig. 2). The atoms involved in the important bonding rearrangements related to discontinuous changes in total energy, force, and conductance are labeled 1–5.

of minimum energy; in this relaxation, only the atoms located in the last two layers remain fixed, meaning that 30 atoms are allowed to relax. The convergence criteria for the relaxation are changes in the total energy per atom less than 10^{-5} eV and forces on the free atoms less than 0.05 eV/Å. We have checked the validity of the calculation performed with FIREBALL96, repeating similar calculations with CASTEP (Ref. 27) at points of the deformation where rearrangement of the atoms appeared (see the discussion below). Figure 1 shows snapshots of the nanowire geometry along the stretching path; different profiles correspond to the points labeled $A-F$ in Fig. 2, where the total energy per atom is shown as a function of the stretching displacement. Figure 2 displays the points where the nanowire suffers an important rearrangement in its geometry: these jumps occur between points B and C, and between points D and E. Figure 1 shows the initial geometry (a), the geometries before and after the first (b),(c) and second (d), (e) jumps, and the structure close to the final breaking point (f). It is important to notice that the main rearrangement of atoms occurs in the layer formed by

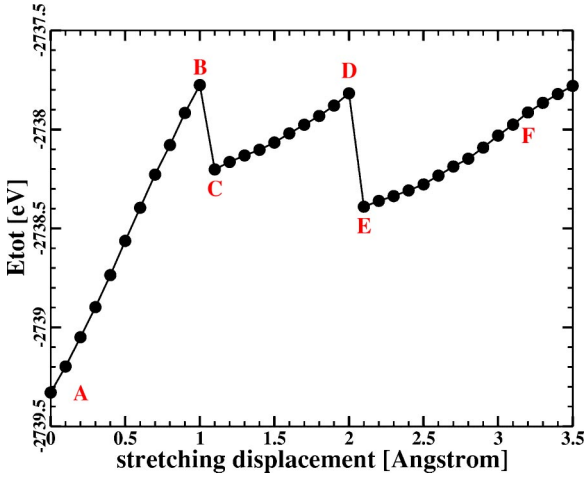

FIG. 2. (Color online) Total energy (per unit cell) of the Al nanowire as a function of the stretching displacement Δd.

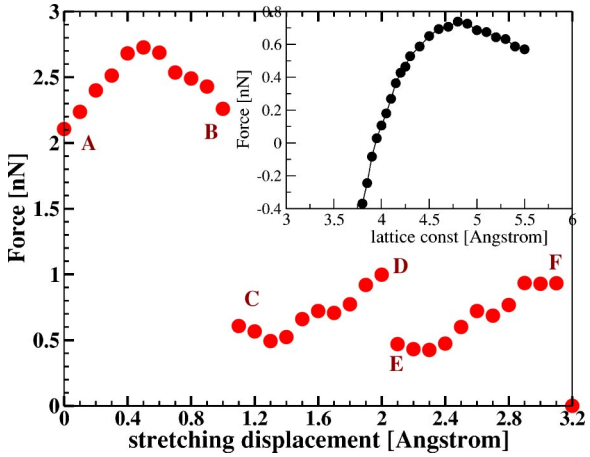

FIG. 3. (Color online) Normal force along the stretching path. The inset shows the force between nearest-neighbour (NN) atoms in Al crystal defined as the derivative of the energy per atom with respect to the NN distance during hydrostatic strain, divided by six bonds assumed in the fcc structure.

atoms 1,2, and 3. In particular, along the path AB, atom 3 starts to move out of the initial 1-2-3 layer; at the first jump, this atom takes an independent position linking a lower layer and the two atoms 1 and 2. Along the path CD, the geometry of the point C does not change too much, atom 2 moving slowly toward atom 3; eventually, at the second jump, atom 2 forms a dimer with atom 3, and the nanowire reaches a geometry very similar to the one formed at the breaking point. In particular, along the EF path the system evolves, basically, changing mostly the distance between atoms 2 and 3.

We have checked these calculations, obtained using a FIREBALL code, by recalculating geometries around the jumps (BC and DE) using CASTEP: these calculations confirm the validity of the FIREBALL results; we have found, however, some minor differences. For instance, in CASTEP we find the system to present the first jump for $\Delta d = 0.9$ Å—namely, a step before the jump found in FIREBALL; the system evolves, however, across the first jump to the same geometry calculated in FIREBALL.

Figure 3 shows the force along the nanowire stretching.[3] Initially, the force is proportional to the displacement (elastic behavior); however, near the first jump, the force saturates and decreases a little due to the plastic deformation of the nanowire. Along the path CD the force increases up to the second jump DE, and along the final deformation EF, the force also increases except for some small fluctuations, until reaching a maximum at the point where the wire breaks. It is interesting to compare the forces shown in Fig. 3 with the one calculated at the break point for an Al crystal: this is defined by the maximum derivative of the energy per atom with respect to the nearest-neighbor distance for an Al crystal, divided by the number of bonds each atom is assumed to form (six bonds per atom in a fcc structure). Our calculations yield 0.7 nN for the maximum force, and this quantity should be compared with the maximum forces in Fig. 3 (the ones found before the structural rearrangements), which are larger than that value: at the nanowire break point the force is around 1.0 nN, 1.4 times the bulk value.

III. CONDUCTANCE AND EIGENCHANNELS

We have calculated the electrical conductance of the nanowire using a Keldysh-Green function approach based on the first-principles tight-binding Hamiltonian obtained from the FIREBALL code at each point of the deformation path. In this formalism, we rewrite this Hamiltonian describing the system as $\hat{H}_1+\hat{H}_2+\hat{T}_{12}$, where the total system is split into two parts 1 and 2, $\hat{T}_{12}$ defining the coupling between both. Typically, we use the thinnest part of the nanowire to define the interface between these two subsystems. Then, the differential conductance[17] is given by

$$G=\frac{dI}{dV}$$
$$=\frac{4\pi e^2}{\hbar}\mathrm{Tr}[\hat{T}_{12}\hat{\rho}_{22}(E_F)\hat{D}^r_{22}(E_F)\hat{T}_{21}\hat{\rho}_{11}(E_F)\hat{D}^a_{11}(E_F)], \tag{1}$$

where $\hat{\rho}_{11}$ and $\hat{\rho}_{22}$ are the density matrices associated with sides 1 and 2, respectively, while

$$\hat{D}^r_{22}=[\hat{1}-\hat{T}_{21}\hat{g}^r_{11}(E_F)\hat{T}_{12}\hat{g}^r_{22}(E_F)]^{-1} \tag{2}$$

and $\hat{D}^a_{11}$ is given by a similar equation; $\hat{g}^r_{11}$ and $\hat{g}^r_{22}$ are the retarded Green function of the decoupled sides 2 and 1. Notice that the 3×3 Al(111) slab [with two-dimensional (2D) periodicity] where the wire is embedded is enough to provide the infinite number of channels needed to represent the electrodes.

Using Eq. (1), we calculate the differential conductance along the stretching deformation (Fig. 4). From this figure we see how this conductance changes dramatically at points B-C and D-E: in both cases the conductance jump coincides with the force jump (Fig. 3) and is determined by the atomic rearrangement the system suffers at those points. The conductance behavior shows two other important features: (i)

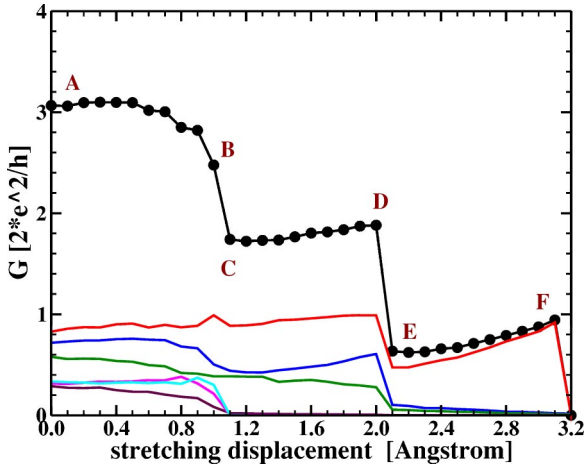

FIG. 4. (Color online) Total differential conductance (in units of the conductance quantum) and channel contribution along the stretching path.

the nanowire breaks at a point where the conductance is very close to the quantum unit, $G \approx 0.95(2e^2/h)$; (ii) second, in the last plateau, the conductance takes values a little smaller than the last one, increasing with the stretching displacement up to the final value reached at the breaking point. These two features are in good agreement with the experimental evidence.[1,28] Morever, at the breaking point the system shows a geometry slightly different to the one suggested in Ref. 5. In particular, we find that an Al dimer is responsible for the conductance properties the nanowire shows before it breaks.

Finally, we have also addressed the question of how many different channels contribute to the conductance. This has also been analyzed using Eq. (1); this equation can be rewritten, using the cyclic property of the trace, in the form[30]

$$G = \frac{dI}{dV} = \frac{2e^2}{h}\mathrm{Tr}(\hat{t}\hat{t}^{+}), \tag{3}$$

where $\hat{t} = 2\pi\hat{\rho}_{11}^{1/2}\hat{D}_{11}^{a}\hat{T}_{12}\hat{\rho}_{22}^{1/2}$. By diagonalizing this transfer matrix, we find the channels contributing to G.

Figure 4 also shows how different channels contribute to the total differential conductance. Near the breaking point, we find that only three channels yield appreciable contributions to the total current, although there appears a predominant mode, very much in agreement with the results published by Scheer *et al.*[5] Along the trajectory CD, before the last jump, the system also presents three predominant channels, but in this case, all the three yield important contributions to the current; notice that in this case the total conductance is around $2(2e^2/h)$, with a channel contributing practically $(2e^2/h)$, and two other channels, each one contributing $\frac{1}{2}(2e^2/h)$. In the initial path, A, B in Fig. 1, we find six channels contributing with a total conductance of around $3(2e^2/h)$. From this analysis we conclude that the channels are not either open or closed; their particular contribution depends very much on the geometry of the nanowire contact. We can only say that channels tend to close along the nanowire deformation and that once a channel is closed by the stretching deformation it remains closed all the time.

IV. DISCUSSION

All the previous *ab initio* calculations for nanowires (with the exception of the work by Nakamura *et al.*[14] for Na nanowires) have assumed model geometries (in particular, for Al, short atomic chains and single-atom contacts) and focused on the calculation of their electronic and transport properties.

At variance with this approach, the whole point of our work is to avoid any educated guess about the geometry of the final stages of the contact: we have performed a lengthy simulation (our calculation represents the largest system—significantly larger in terms of the number of electrons—analyzed up to this moment using DFT techniques) of the whole breaking process in order to identify the structure of the nanocontact during the last stages of the deformation process. This is motivated by what the previous literature on Al nanocontacts tells us: depending on the assumed ideal geometry, even for a single-atom contact, one can have quite different values of the conductance: one quantum of conductance for the single-atom contact between two pyramids,[5,28,29] two conductance quantums for an atom sandwiched between two flat surfaces,[10,11] and an intermediate value for a three-atom chain linked to jellium electrodes (with conductance variations depending on whether there is a triangular atomic basis to make the link or not).[12,13] Although these structures may be stable, no one has shown, up to now, that they are likely to appear during stretching of a real contact.

Thus, we are still at the stage where understanding of the basic processes determining the transport properties and, in particular, their correlation with structural transformations in the nanocontact is the basic goal. Unfortunately, approximate total-energy methods—based on fits to bulk properties—are not reliable enough for this task and one has to resort to time-consuming first-principles DFT calculations. This precludes a full statistical calculation of the conductance properties, but notice that the experiments we are addressing are performed at very low temperatures (few K),[5,28] where a total-energy calculation would provide a fair representation of the stable structures.

Following this approach, we have let the nanowire evolve during the stretching process and have calculated the corresponding transport properties. The combination of our local orbital basis formulation of DFT and the Keldish nonequilibrium formalism allows a direct determination of the transport properties from the electronic Hamiltonian for each step of the breaking process, without the further approximations needed to extract transport properties from *ab initio* approaches based on the plane-wave basis (see, for example, Ref. 14).

It is the interplay between the stable geometric structures and the associated electronic properties that determines the calculated conductance properties. Thus, one has to be very careful when comparing our results with previous model cal-

culations. Notice that atomic arrangements such as *C* and *D* in our calculation differ from the ideal single-atom contact assumed by many authors. For example, in Ref. 29 the central atom is linked to two three-atom fcc planes rotated with respect to each other in a particularly symmetric arrangement [two perfect (111)-oriented fcc pyramids] with inversion symmetry, while in our calculations atom 3 is linked to three atoms in one side and two atoms (atoms 1 and 2; see Fig. 1). We cannot see any contradiction between the conductance results given the different geometries considered.

Furthermore, the dimer geometry we have found for the nanocontact structure before the final breaking nicely reproduces the presence of three conducting channels, one with a dominant contribution, giving the total conductance close to the quantum of conductance found in the experiments. However, it differs significantly from all the assumed geometries discussed in the literature and, in particular, from the ideal single-atom contact. The fact that we also reproduce the characteristic increase of the conductance in the last plateau (not found in any previous *ab initio* study) indicates that the geometry found in our calculation is a fair representation of the deformation appearing near the breaking of the nanocontact.

V. CONCLUSION

We have presented total-energy DFT and conductance calculations for the stretching deformation of an Al nanowire. The use of a fast local-orbital code has allowed us to analyze in detail the nanowire geometrical configurations along the stretching path. At the same time, the first-principles tight-binding Hamiltonian obtained at each geometry for the electronic system has allowed us to analyze also in a direct and very efficient way, using Keldysh-Green function methods, the differential conductance of the system. Our results reproduce most of the experimental evidence—in particular, the increase of the conductance in the last plateau—and show that the deformation induces at particular points sudden rearrangement of atoms that manifest itself in jumps of the forces and the conductance. We also find that in the final process of deformation, the nanowire does not form a single-atom contact but adopts a dimer geometry and breaks at a point having a differential conductance close to $(2e^2/h)$. The total conductance in these last stages is the result of the contribution of three channels, one of them being the predominant one.

ACKNOWLEDGMENTS

P.J. gratefully acknowledges financial support by European Project No. HPRN-CT-2000-00154. This work has been supported by the DGI-MCyT (Spain) under Contract No. MAT2001-0665 and by Consejeria de Educación de la Comunidad de Madrid under Project No. 07N/0050/2001.

[1] N. Agräit, A. Levy-Yeyati, and J. van Ruitenbeek, Phys. Rep. **377**, 81 (2003).
[2] G. Rubio-Bollinger, N. Agräit, and S. Vieira, Phys. Rev. Lett. **76**, 2302 (1996).
[3] G. Rubio-Bollinger *et al.*, Phys. Rev. Lett. **87**, 026101 (2001).
[4] E. Scheer, N. Joyez, D. Esteve, C. Urbina, and M.H. Devoret, Phys. Rev. Lett. **78**, 3535 (1997).
[5] E. Scheer, N. Agräit, J.C. Cuevas, A. Levy Yeyati, B. Ludoph, A. Martín-Rodero, G.R. Bollinger, J.M. van Ruitenbeek, and C. Urbina, Nature (London) **394**, 154 (1998).
[6] U. Landman, W.D. Ludetke, B.E. Salisbury, and R.L. Whetten, Phys. Rev. Lett. **77**, 1362 (1996).
[7] T.N. Todorov and A.P. Sutton, Phys. Rev. Lett. **70**, 2138 (1993).
[8] A.M. Bradkovsky, A.P. Sutton, and T.N. Todorov, Phys. Rev. B **52**, 5036 (1995).
[9] M.R. Sörensen, M. Brandbyge, and K.W. Jacobsen, Phys. Rev. B **57**, 3283 (1998).
[10] N.D. Lang, Phys. Rev. B **52**, 5335 (1995).
[11] C.C. Wan, J.-L. Mozos, G. Taraschi, J. Wang, and H. Guo, Appl. Phys. Lett. **71**, 419 (1997).
[12] N. Kobayashi, M. Brandbyge, and M. Tsukada, Phys. Rev. B **62**, 8430 (2000).
[13] N. Kobayashi, M. Brandbyge, and M. Tsukada, Surf. Sci. **433-435**, 854 (1999).
[14] A. Nakamura, M. Brandbyge, L.B. Hansen, and K.W. Jacobsen, Phys. Rev. Lett. **82**, 1538 (1999).
[15] K. Hirose and M. Tsukada, Phys. Rev. B **51**, 5278 (1995).
[16] D. Krüger, H. Fuchs, R. Rousseau, D. Marx, and M. Parrinello, Phys. Rev. Lett. **89**, 186402 (2002).
[17] N. Mingo, L. Jurczyszyn, F.J. GarciaVidal, R. SaizPardo, P.L. de Andres, F. Flores, S.Y. Wu, and W. More, Phys. Rev. B **54**, 2225 (1996).
[18] A. Demkov, J. Ortega, O.F. Sankey, and M.P. Grumbach, Phys. Rev. B **52**, 1618 (1995).
[19] O.F. Sankey and D.J. Niklewski, Phys. Rev. B **40**, 3979 (1989).
[20] The valence electrons were described by *s* and *p* slightly excited pseudoatomic orbitals (Ref. 19). For the cutoff radii $R_c = 6.4$ a.u. we obtained for fcc Al a lattice parameter of $a = 3.97$ Å and a bulk modulus of $B = 74$ GPa (experiment: $a = 4.05$ Å, $B = 76$ GPa).
[21] Computer code CASTEP 4.2 academic version, licensed under the UKCP-MSI Agreement, 1999; M.C. Payne *et al.*, Rev. Mod. Phys. **64**, 1045 (1992).
[22] G. Taraschi, J.-L. Mozos, C.C. Wan, H. Guo, and J. Wang, Phys. Rev. B **58**, 13 138 (1998).
[23] H. Mehrez, A. Wlasenko, B. Larade, J. Taylor, P. Grutter, and H. Guo, Phys. Rev. B **65**, 195419 (2002).
[24] M. Brandbyge, J.-L. Mozos, P. Ordejon, J. Taylor, and K. Stokbro, Phys. Rev. B **65**, 165401 (2002).
[25] J.J. Palacios, A.J. Perez-Jimenez, E. Louis, E. SanFabian, and J.A. Verges, Phys. Rev. B **66**, 035322 (2002).
[26] J. Heurich, J.C. Cuevas, W. Wenzel, and G. Schön, Phys. Rev. Lett. **88**, 256803 (2002).
[27] We use an ultrasoft pseudopotential [D. Vanderbilt, Phys. Rev. B **41**, 7892 (1990)] for Al, which produces converged results

with the 100 eV cutoff used in our calculations.

[28] J.C. Cuevas, A. Levy Yeyati, A. Martin-Rodero, G. Rubio Bollinger, C. Untiedt, and N. Agraït, Phys. Rev. Lett. **81**, 2990 (1998).

[29] J.C. Cuevas, A. Levy Yeyati, and A. Martin-Rodero, Phys. Rev. Lett. **80**, 1066 (1998).

[30] M. Büttiker, Y. Imry, R. Landauer, and S. Pinhas, Phys. Rev. B **31**, 6207 (1985).